

# Mitochondria-derived nuclear ATP surge protects against confinement-induced proliferation defects

Ritobrata Ghose<sup>1,2,10,†</sup>, Fabio Pezzano<sup>1,†</sup>, Rémi Badia<sup>1</sup>, Savvas Kourtis<sup>1</sup>, Ilir Sheraj<sup>1</sup>, Shubhamay Das<sup>1</sup>, Antoni Gañez Zapater<sup>1</sup>, Upamanyu Ghose<sup>3</sup>, Sara Musa-Afaneh<sup>1</sup>, Lorena Espinar<sup>1</sup>, Albert Coll-Manzano<sup>1</sup>, Katja Parapatics<sup>4</sup>, Saška Ivanova<sup>5,6,7</sup>, Paula Sánchez-Fernández-de-Landa<sup>5,6,7</sup>, Dragana Radivojević<sup>5,6,7</sup>, Valeria Venturini<sup>1</sup>, Stefan Wieser<sup>8</sup>, Antonio Zorzano<sup>5,6,7</sup>, André C Müller<sup>4</sup>, Verena Ruprecht<sup>1,2,8,\*</sup>, Sara Sdelci<sup>1,2,9,\*</sup>

<sup>1</sup>Centre for Genomic Regulation (CRG), The Barcelona Institute of Science and Technology; Barcelona 08003, Spain

<sup>2</sup>Universitat Pompeu Fabra (UPF); Barcelona 08002, Spain

<sup>3</sup>Department of Psychiatry, University of Oxford; Oxford OX3 7JX, United Kingdom

<sup>4</sup>CeMM Research Center for Molecular Medicine of the Austrian Academy of Sciences; Vienna 1090, Austria

<sup>5</sup>Institute for Research in Biomedicine (IRB Barcelona), The Barcelona Institute of Science and Technology, Carrer Baldri Reixac 10, 08028 Barcelona, Spain

<sup>6</sup>Departament de Bioquímica i Biomedicina Molecular, Facultat de Biologia, Universitat de Barcelona, Barcelona, Spain

<sup>7</sup>Centro de Investigación Biomédica en Red de Diabetes y Enfermedades Metabólicas Asociadas (CIBERDEM) Instituto de Salud Carlos III, Madrid, Spain

<sup>8</sup>University of Innsbruck, Innrain 52, 6020 Innsbruck, Austria

<sup>9</sup>Lead contact

<sup>10</sup>Current affiliation: The Breast Cancer Now Toby Robins Research Centre, The Institute of Cancer Research, London, UK

† These authors contributed equally

\*Correspondence: [sara.sdelci@crg.eu](mailto:sara.sdelci@crg.eu); [verena.ruprecht@crg.eu](mailto:verena.ruprecht@crg.eu)

## CONTENTS

### Supplementary Figures

Figure S1. Related to Figure 1. Quality control for subcellular fractionation and proteomics.

Figure S2. Related to Figure 2. Characterisation of NAM and nuclear indentations.

Figure S3. Related to Figure 3. NAM regulation by actin and mitochondrial fission and fusion.

Figure S4. Related to Figure 3. Mitochondrial co-localization with various organelles.

Figure S5. Related to Figure 4. Nuclear and mitochondrial ATP.

Figure S6. Related to Figure 5. Nuclear ATP regulates chromatin compaction under confinement.

Figure S7. Related to Figure 6. DNA damage and cell cycle.

### Supplementary Tables

Supplementary Table 1: ATAC-seq library preparation multiplexing adaptors.

### Supplementary References

### Western Blots

All uncropped Western Blots relevant to main and supplementary figures.

## SUPPLEMENTARY FIGURES

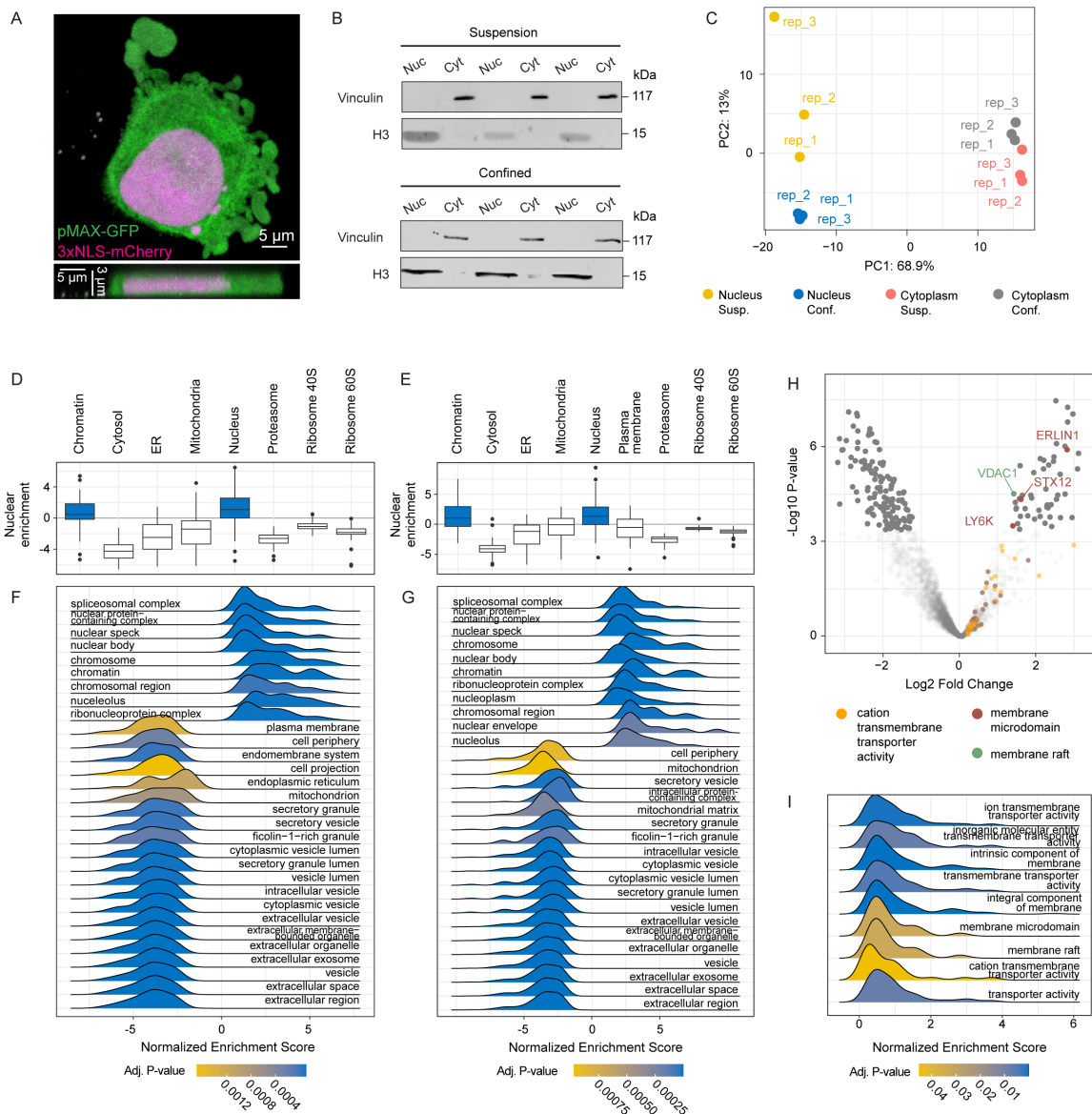


**Figure S1. Related to Figure 1. Quality control for subcellular fractionation and proteomics.**

(A) HeLa cells displaying blebs when confined to a height of approximately 3  $\mu\text{m}$  using the confinement system depicted in Figure 1 A.

(B) Western blots to validate nucleo-cytoplasmic fractions of three independent samples obtained through subcellular fractionation of HeLa cells in suspension or confinement. H3 antibody and Vinculin antibodies were used to test nuclear and cytoplasmic fractions, respectively.

(C) PCA of results obtained from MS showing clustering among replicates and a clear separation between and within fractions (nucleus vs cytoplasm) and conditions (confinement vs suspension).

(D-E) Enriched and depleted terms when comparing the nuclear vs cytoplasmic fraction of suspension HeLa cells (D) or acutely confined HeLa cells (E). Enrichment of chromatin and nuclear terms, and depletion of cytosolic and other organelle terms confirms successful nucleo-cytoplasmic fractionation of suspension and confined cells.

(F) GSEA of proteins from the nucleus-cytoplasm comparison of suspension cells shown in (D). P-values are FDR adjusted.

- (G)** GSEA of proteins from the nucleo-cytoplasmic comparison of acutely confined cells shown in (E). P-values are FDR adjusted.
- (H)** Enriched and depleted terms when comparing the cytoplasmic fraction of confined HeLa cells to that of unconfined cells.
- (I)** Comparison of GSEA performed on the cytoplasmic fractions in (I) only revealed membrane transport activity-related terms. P-values are FDR adjusted.

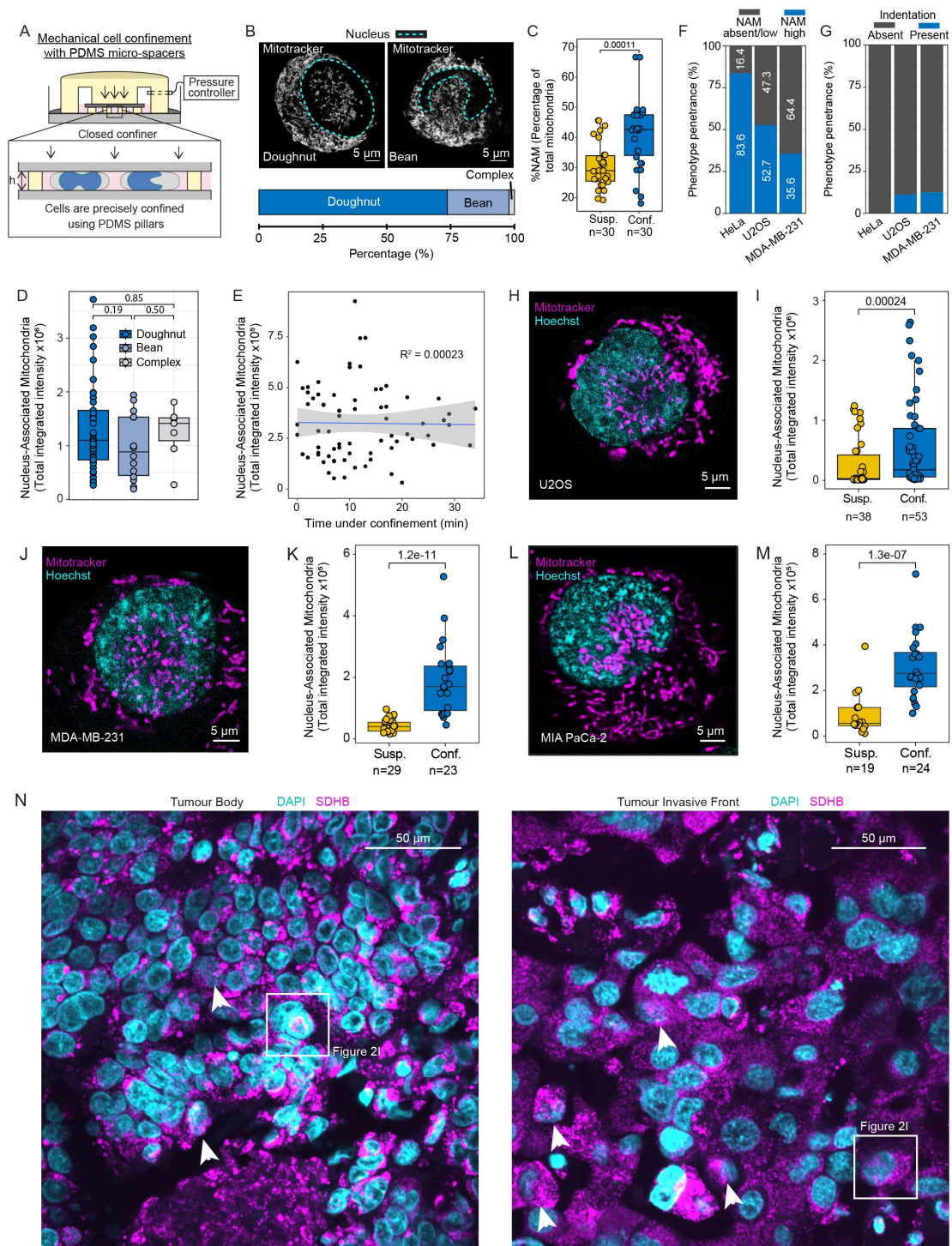


**Figure S2. Related to Figure 2. Characterisation of NAM and nuclear indentations.**

(A) Schematic of pressurised dynamic confinement system using 3  $\mu$ m PDMS microspacers to control confinement height. Adapted from 4DCell<sup>1</sup>.

(B) Proportion of nuclear indentations, “doughnuts”, “beans”, or complex, in cells positive for nucleus-associated mitochondria (NAM), based on Hoechst and mitochondrial localisation.

(C) NAM levels expressed as percentage of total mitochondria per cell. NAM segmented around the nuclear region as in Fig. 2E. Each dot represents one cell (n as indicated).

(D) NAM levels in acutely confined HeLa cells grouped by nuclear shape. n indicates cells analysed.

(E) NAM levels in HeLa cells during confinement (n = 73). Line indicates linear regression; shaded band indicates 95% confidence interval ( $R^2 = 0.00023$ ).



**(F)** Penetrance of NAM in confined HeLa, U2OS and MDA-MB-231 cells. Quantified from maximum intensity projections..

**(G)** Proportion of nuclear indentations in ‘NAM absent/low’ confined cells across HeLa, U2OS and MDA-MB-231 cell lines.

**(H, J, L)** Representative image of confined (H) U2OS, (J) MDA-MB-231 and (L) MIA PaCa-2 cells stained with Hoechst (nucleus) and MitoTracker (mitochondria).

**(I, K, M)** NAM quantification in U2OS cells in suspension and acute confinement. Each dot represents one cell (n as indicated).

**(N)** Immunofluorescence of breast cancer tissue microarray (TMA; tumours from 17 individuals) comparing tumour body (N=8) and invasive front (N=9). Stained for SDHB (mitochondria) and DAPI (nuclei). Boxes mark NAM-high cells shown in Figure 2I; arrows indicate additional NAM-high cells.

Statistics in (C, D, I, K, M) were calculated by Wilcoxon-Mann-Whitney test. Box plots show lower quartile, median and upper quartile; whiskers indicate minimum and maximum.

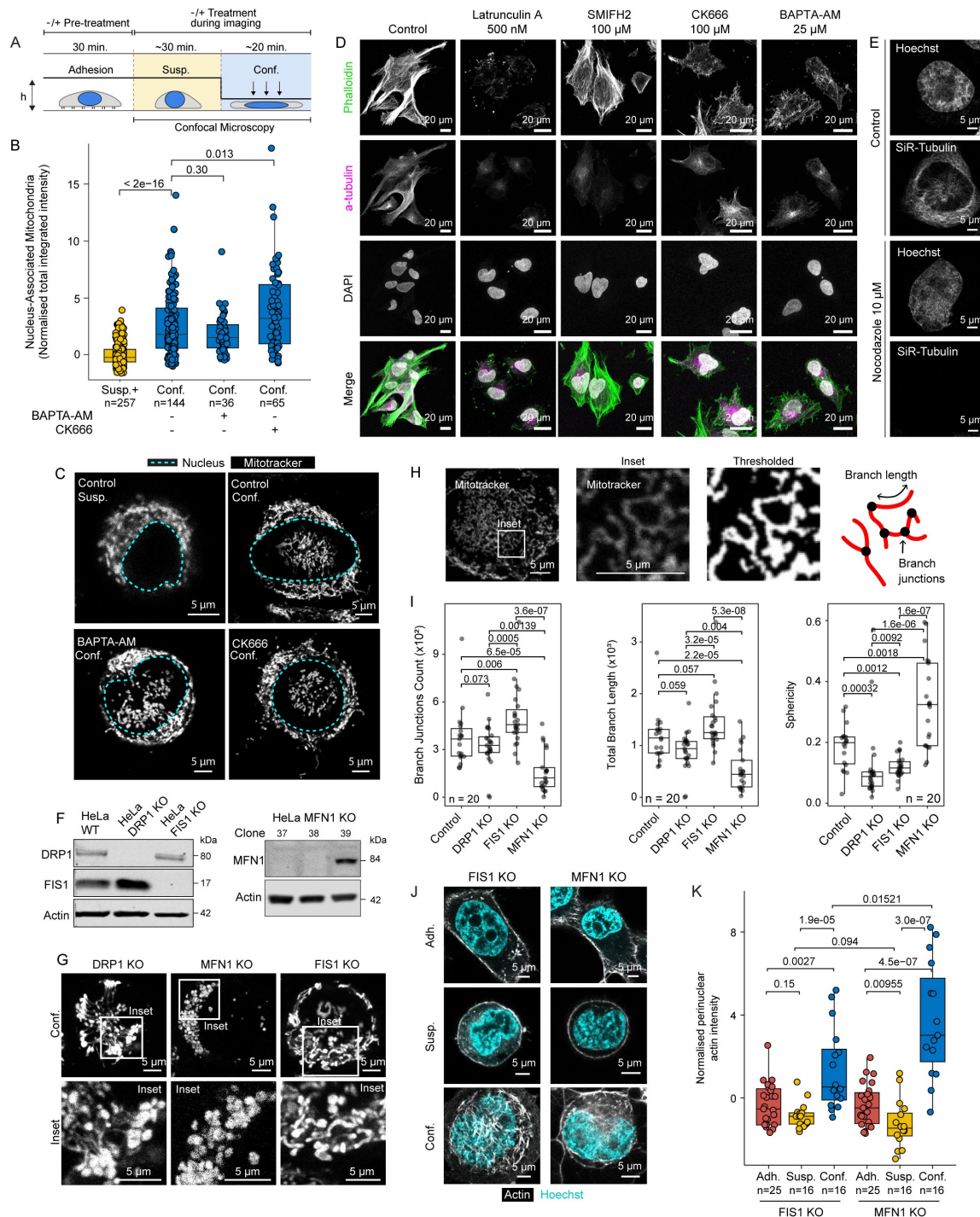


**Figure S3. Related to Figure 3. NAM regulation by actin and mitochondrial fission and fusion.**

(A) Experimental workflow for pharmacological treatment and acute confinement imaging. Cells were treated with a pharmacological agent for 30 minutes, then confocal images of suspension cells followed by acutely confined cells was acquired.

(B) NAM quantification in HeLa cells treated with CK-666 (100  $\mu$ M) and BAPTA-AM (10  $\mu$ M) using zero mean normalization. Data shown here were normalised together with data in Figure 3 A. Each point represents a cell, and n indicates the total number of cells analysed.

(C) Representative HeLa images corresponding to CK-666 (100  $\mu$ M) and BAPTA-AM (10  $\mu$ M) treatments in (B). Mitochondria were stained with MitoTracker and nuclei were outlined based on the Hoechst signal.

**(D)** Immunofluorescent images of fixed adherent HeLa cells stained with Phalloidin (actin),  $\alpha$ -Tubulin (microtubule), or DAPI (nucleus). Cells were treated with Latrunculin A (500 nM), BAPTA-AM (25  $\mu$ M) or CK-666 (100  $\mu$ M) for 30 min, or SMIFH2 (100  $\mu$ M) for 1 hour.

**(E)** Representative HeLa images corresponding to control and Nocodazole (10  $\mu$ M) treatment. Microtubules were stained with SiR-Tubulin and nuclei with Hoechst.

**(F)** Western blot validation of HeLa DRP1 KO, FIS1 KO, and MFN1 KO (clone 37 was used).

**(G)** Representative mitochondrial morphology (MitoTracker) in confined HeLa DRP1 KO, FIS1 KO, and MFN1 KO cells.

**(H-I)** Morphology analysis pipeline to assess branch length, number of branch junctions, and sphericity of mitochondria in HeLa wild-type, DRP1 KO, MFN1 KO and FIS1 KO cell lines in confinement. Each data point is a cell (n indicated).

**(J)** Representative images of actin (SiR-Actin) and nuclei (Hoechst) in FIS1 KO and MFN1 KO HeLa cells, in adhesion, suspension or confinement.

**(K)** Perinuclear actin in a ring region around the nucleus in FIS1 KO and MFN1 KO HeLa cells normalised to the respective adhesion conditions. Analysis was performed on individual z-slices of a cell and averaged per cell (n is indicated).

Statistics in (B, I, K) are Wilcoxon-Mann-Whitney test to compare means. Box plots show lower quartile, median and upper quartile. Whiskers represent the minimum and maximum.

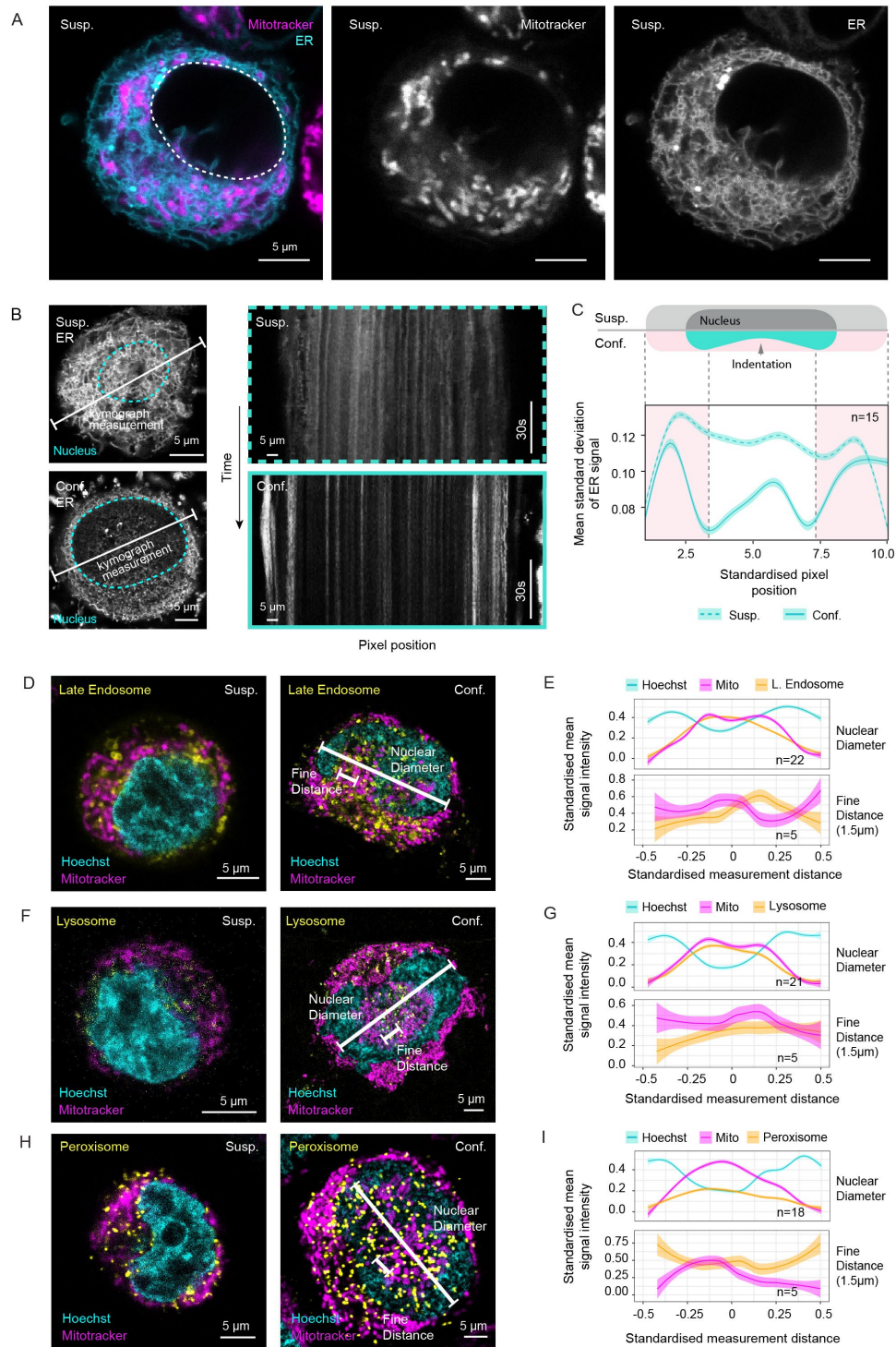


**Figure S4. Related to Figure 3. Mitochondrial co-localization with various organelles.**

(A) Suspension HeLa cells tagged with MitoTracker and expressing a Turquoise-tagged ER-localising KDEL. Dashed white line represents the nucleus.

(B) Kymographs generated from line profiles of ER (Turquoise KDEL) signal on the basal plane of suspension and confined HeLa cells that are shown. Dashed cyan line represents the nucleus. Kymograph measurement was performed for line profiles spanning the cell diameter and measured over 70 seconds.

(C) Quantification of the dynamicity of ER signal based on kymographs of suspension or confined HeLa cells (n = 15), as shown in (B). Dynamicity was quantified as the standard deviation of ER signal

per pixel on the x axis. Signal dispersion was depicted as mean standard deviation along with their 95% confidence interval. n indicates the total number of cells analysed.

**(D, F, H)** Representative images of suspension and confined HeLa cells stained for mitochondria (MitoTracker), nuclei (Hoechst) and (D) late endosomes (CellLight BacMam 2.0), (F) lysosomes (LysoTracker), and (H) peroxisomes (CellLight BacMam 2.0). White lines in confined cells indicate where measurements were performed for the line profiles in (E, G, I).

**(E, G, I)** Line profiles showing the localisation of either (E) late endosomes (CellLight BacMam 2.0), (G) lysosomes (LysoTracker), or (I) peroxisomes (CellLight BacMam 2.0) with respect to either mitochondria across the nuclear diameter, or with respect to mitochondria along a 1.5  $\mu\text{m}$  long line (“Fine Distance”) starting at a point of high mitochondrial signal. See representative lines in (D, F, H). Measuring distances and intensity of signal were centred and standardized across multiple cells. n represents the total number of cells analysed. Dark lines represent a best fit generalized additive model, and the shaded band represents 95% confidence interval.



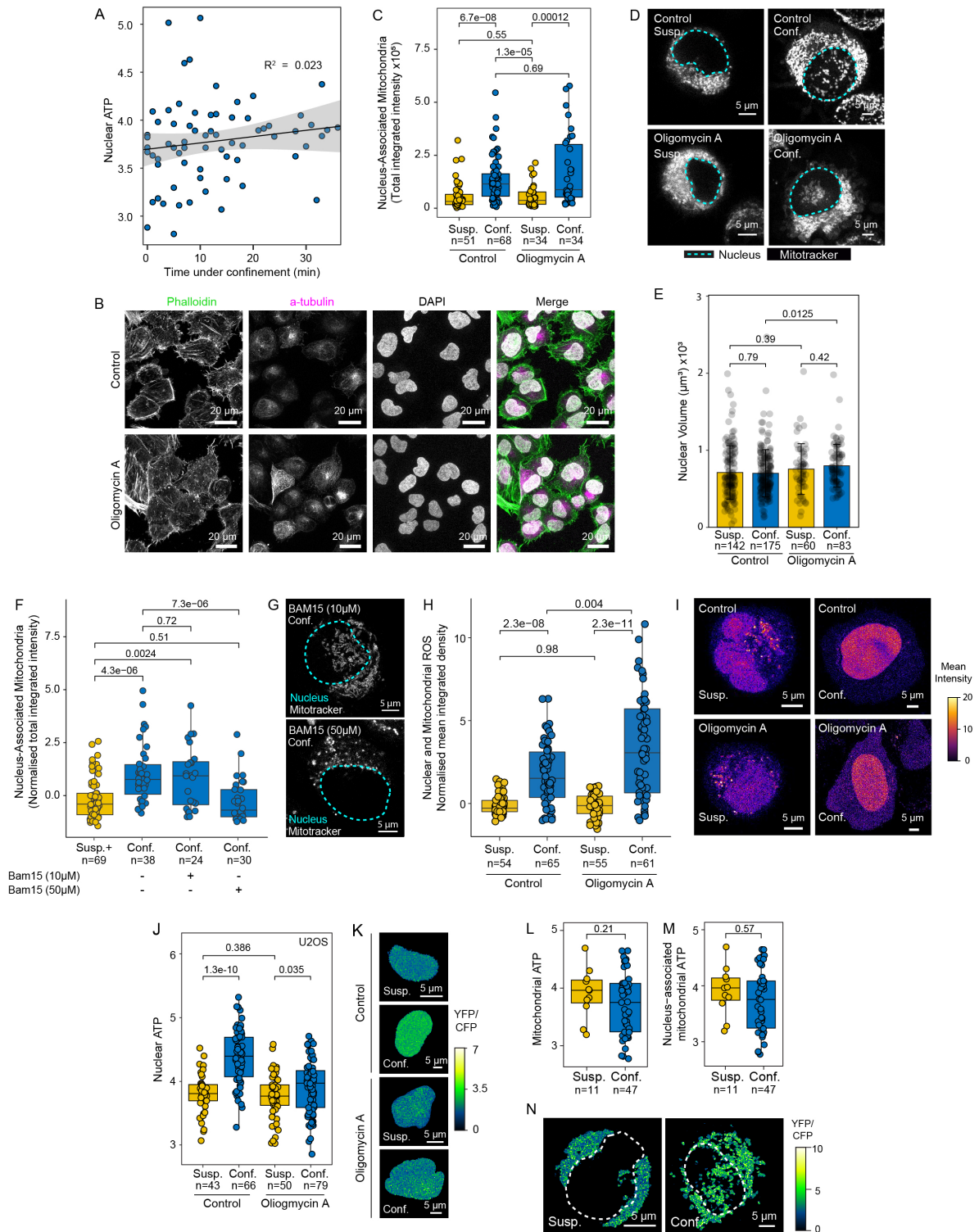


**Figure S5. Related to Figure 4. Nuclear and mitochondrial ATP.**

**(A)** Correlation between nuclear ATP levels and confinement time with linear regression fit and 95% confidence interval ( $n = 25$ ,  $R^2 = 0.023$ ).

**(B)** Immunofluorescence images of fixed HeLa cells stained for actin (Phalloidin), microtubules ( $\alpha$ -Tubulin), and nuclei (DAPI) following a 30-minute Oligomycin A (1  $\mu$ M) treatment.

**(C)** NAM quantification (zero mean normalised) in control or Oligomycin A (1  $\mu$ M) treated HeLa cells. Each data point is a cell ( $n$  indicated).

**(D)** Representative images of mitochondria (MitoTracker in grey) and nuclei (based on Hoechst) of cells quantified in (C).

**(E)** Nuclear volume of HeLa cells in indicated conditions. Each point represents a cell (n indicated).

**(F)** NAM quantification (zero mean normalised) in HeLa cells treated with BAM15 at 10  $\mu$ M and 50  $\mu$ M. Each data point is a cell (n indicated).

**(G)** Representative images of mitochondria (MitoTracker in grey) and nuclei (based on Hoechst) of cells quantified in (F).

**(H)** Quantification of nuclear and mitochondrial ROS (CellROX Green) in HeLa cells in suspension or confinement, either untreated or treated with Oligomycin A (1  $\mu$ M). ROS levels are shown as normalised integrated intensity, averaged across z-slices. Each point represents a cell (n indicated).

**(I)** Representative ROS images of HeLa cells quantified in (H). CellROX Green shows both nuclear and mitochondrial ROS.

**(J)** Nuclear ATP quantification in U2OS cells with or without Oligomycin A (1  $\mu$ M) treatment. Each point represents a cell (n indicated).

**(K)** Representative images of the YFP/CFP ratio showing nuclear ATP in U2OS cells as quantified in (J).

**(L-M)** Quantification of whole-cell mitochondrial ATP levels (L) and NAM-specific ATP levels (M) in suspension and confined HeLa cells using a FRET-based mitochondrial ATP sensor<sup>2</sup>.

**(N)** Representative images of the YFP/CFP ratio showing mitochondrial ATP in U2OS cells as quantified in (L-M). Dashed white lines represent the nucleus.

Statistics in (C, E, F, H, J, L, M) are Wilcoxon-Mann-Whitney test to compare means. Box plots represent the lower quartile, median and upper quartile. Whiskers represent the minimum and maximum.

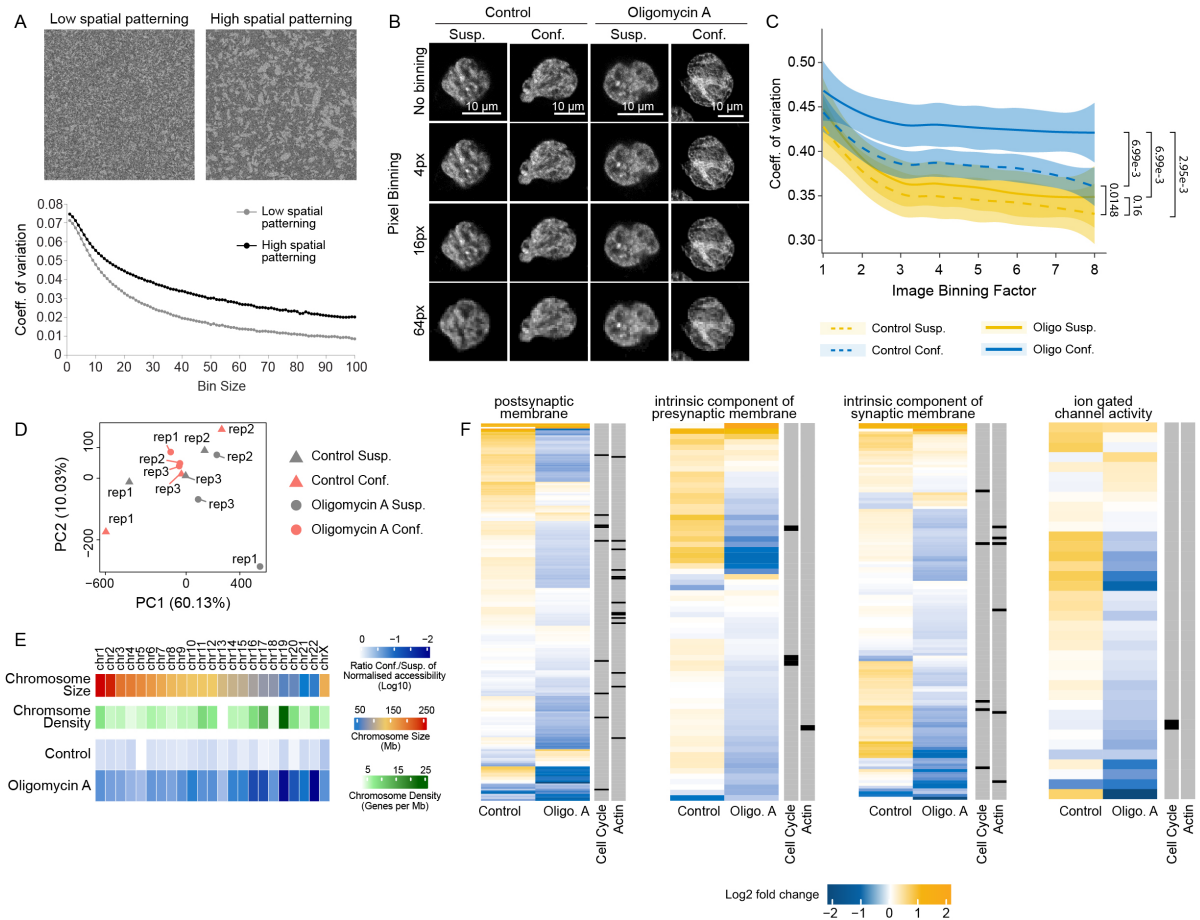


**Figure S6. Related to Figure 5. Nuclear ATP regulates chromatin compaction under confinement.**

**(A)** Quantification of computationally simulated images of chromatin structure with a controlled spatial heterochromatin and euchromatin distribution. Low spatial patterning represents a more dispersed organization of heterochromatin regions, while high spatial patterning shows concentrated domains of heterochromatin. Quantification of chromatin compaction was derived as the coefficient of variation (standard deviation / mean) of the image signal, using 20 images per condition.

**(B)** Maximum projection of the three central z planes of Hoechst-stained nuclei in HeLa cells, either in suspension or acutely confined cells, and untreated or treated with Oligomycin A (1  $\mu$ M). Signal intensities were progressively binned up to 8x8 bins (64 pixels). For the figure, all images were rescaled to the same size for visual consistency, regardless of the binning level.

**(C)** Quantification of chromatin compaction as coefficient of variation (standard deviation / mean) of Hoechst signal from nuclei as in (B). Dark lines correspond to best fit line using a generalized additive model, and shaded areas correspond to the 95% confidence intervals for  $n > 15$  cells per condition. Statistical analysis was performed using the Wilcoxon-Mann-Whitney test to compare the distribution/ranks of the groups.

**(D)** Principal component analysis of ATAC sequencing data for suspension and confined HeLa cells either treated or untreated with Oligomycin A (1  $\mu$ M).

**(E)** Ratio for confinement/suspension of the normalised peak count per chromosome. Normalisation was done against chromosome size. Chromosome size (Mb) and chromosome gene density (genes per Mb) are also shown.

**(F)** Log2 fold change of genes detected in the ATAC-Seq dataset corresponding to the gene ontology GO:0099240 intrinsic component of synaptic membrane, GO:0098889 intrinsic component of

presynaptic membrane, GO:0045211 postsynaptic membrane, and GO:0022839 ion gated channel activity, as enriched in Figure 5 G. Annotations in black highlight genes belonging to either actin cytoskeleton organisation (GO:0030036) or the cell cycle (GO:0007049).

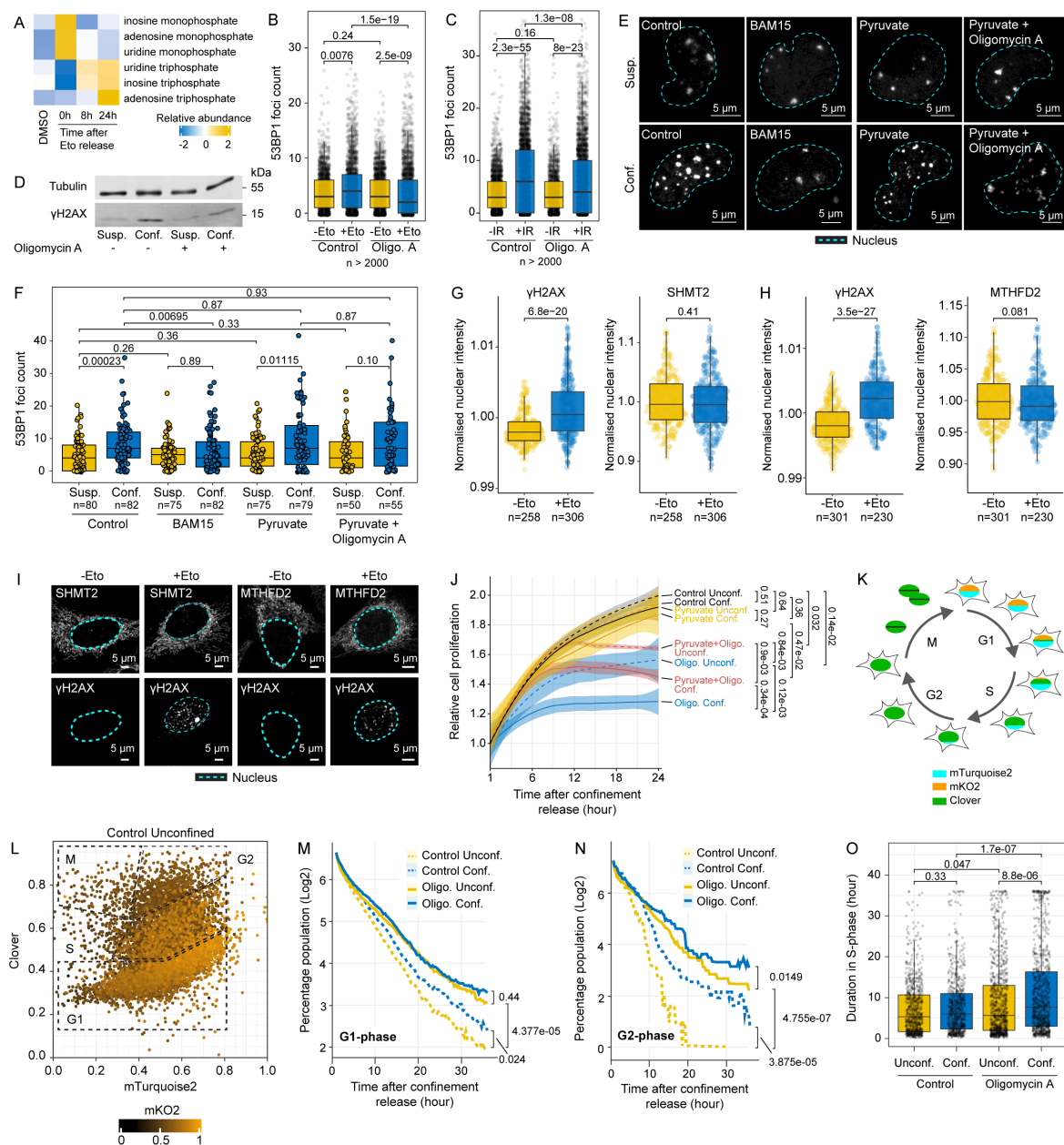


**Figure S7. Related to Figure 6. DNA damage and cell cycle.**

(A) Targeted metabolomics profiling after treatment of U2OS cells with DMSO or etoposide (1  $\mu$ M) for 3 h, and following 0 h, 8 h, and 24 h post-treatment release.

(B) Quantification of 53BP1 foci in U2OS cells treated with DMSO or etoposide (1  $\mu$ M) for 3 h in the presence or absence of Oligomycin A (1  $\mu$ M).

(C) Quantification of 53BP1 foci in untreated or  $\gamma$ -irradiated, control or Oligomycin A-treated U2OS cells.

(D) Western blot of  $\gamma$ H2AX in control or Oligomycin A-treated suspension and confined HeLa cells.  $\alpha$ -Tubulin was used as loading control.

(E) Representative images of 53BP1 foci in U2OS cells expressing a truncated-53BP1-maroon reporter. Cells are either untreated or treated with BAM15 (10  $\mu$ M), pyruvate (3 mM) and pyruvate + Oligomycin A (3 mM + 1  $\mu$ M respectively). Images are maximum intensity projections and show nuclear outline based on transmitted light.



**(F)** 53BP1 foci count on maximum intensity projection images as in (E). Each point represents a cell (n indicated).

**(G-H)** Quantification of DNA damage ( $\gamma$ H2AX) and NAM (SHMT in G, MTHFD2 in H in the nuclear ROI) in HeLa cells treated with DMSO or etoposide (1  $\mu$ M) for 3 h.

**(I)** Representative images of HeLa cells treated with DMSO or etoposide (1  $\mu$ M), stained for  $\gamma$ H2AX, SHMT2 and MTHD2 as quantified in (G-H). Images are single plane, and the outline of the nucleus is based on DAPI.

**(J)** Relative cell proliferation of U2OS cells under confinement with Oligomycin A (1  $\mu$ M), pyruvate (3 mM), or combined treatments. Lines show generalized additive model fits with 95% confidence intervals. Oligomycin A data from Figure 6G. At timepoint 1, average n = 2000 for three biological replicates.

**(K)** FUCCI cells expressing SLBP-Turquoise2, Clover-Geminin, Cdt1-mKO2 enable cell cycle analysis using the gating strategy in **(L)**.

**(M-N)** Progression of cells detected in the G1-phase (M) or G2-phase (N) after confinement release. Data is mean of three biological replicates.

**(O)** Time taken by cells detected in S-phase post-confinement release to progress through S-phase. Statistics in (B, C, F, G, H, O) are Wilcoxon-Mann-Whitney test to compare the means. Statistics in (J, M, N) are Wilcoxon test to compare the distribution/ranks of the groups. Box plots represent the lower quartile, median and upper quartile. Whiskers represent the minimum and maximum.

## SUPPLEMENTARY REFEEENCES

1. Le Berre, M., Aubertin, J. & Piel, M. Fine control of nuclear confinement identifies a threshold deformation leading to lamina rupture and induction of specific genes. *Integrative Biology* 4, 1406 (2012).
2. Imamura, H. *et al.* Visualization of ATP levels inside single living cells with fluorescence resonance energy transfer-based genetically encoded indicators. *Proc Natl Acad Sci U S A* 106, 15651–15656 (2009).

## SUPPLEMENTARY TABLES

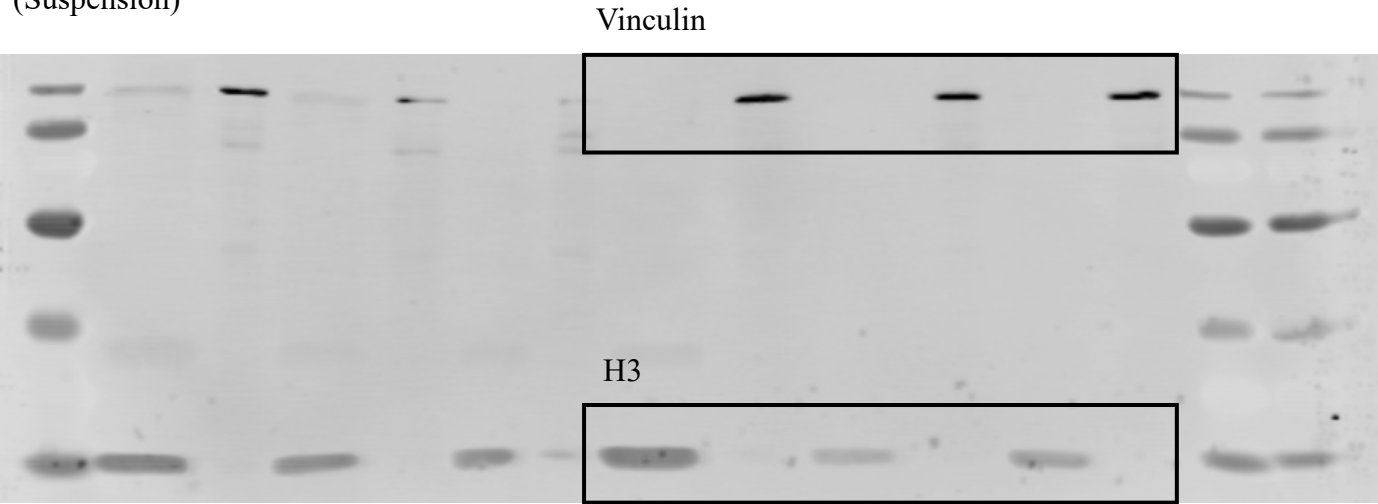
**Supplementary Table 1: ATAC-seq library preparation multiplexing adaptors**

Replication/Treatment/Confinement	Sample name	Multiplex Index P7	Multiplex Index P5
Replicate 1 Untreated Suspension	n4_UU	TAAGGCGA	TAGATCGC
Replicate 1 Untreated Confined	n4_CU	CGTACTAG	CTCTCTAT
Replicate 1 Treated Suspension	n4_UT	AGGCAGAA	TATCCTCT
Replicate 1 Treated Confined	n4_CT	TCCTGAGC	AGAGTAGA
Replicate 2 Untreated Suspension	n5_UU	GGACTCCT	GTAAGGAG
Replicate 2 Untreated Confined	n5_CU	TAGGCATG	ACTGCATA
Replicate 2 Treated Suspension	n5_UT	CTCTCTAC	AAGGAGTA
Replicate 2 Treated Confined	n5_CT	CGAGGCTG	CTAAGCCT
Replicate 3 Untreated Suspension	n3_UU	AAGAGGCA	CGTCTAAT
Replicate 3 Untreated Confined	n3_CU	GTAGAGGA	TCTCTCCG
Replicate 3 Treated Suspension	n3_UT	GCTCATGA	GAGCCTTA
Replicate 3 Treated Confined	n3_CT	ATCTCAGG	TTATGCGA

WESTERN BLOT RAW DATA

Figure S1 B

(Suspension)



(Confined)

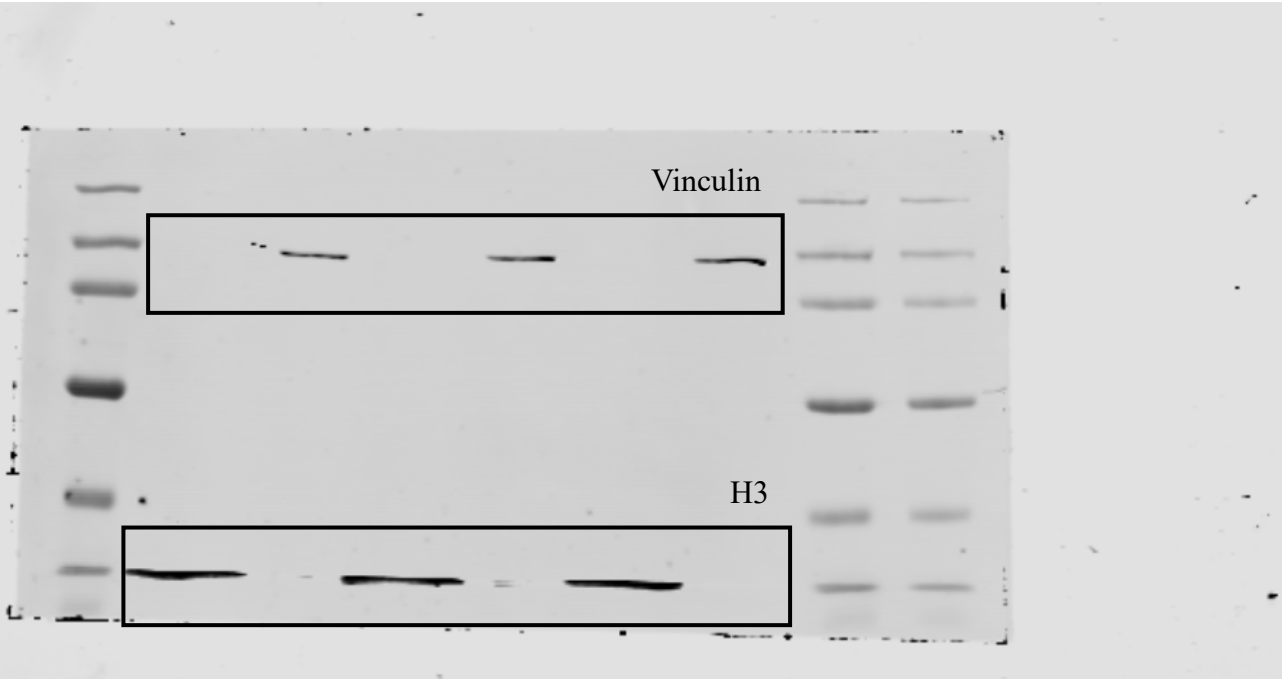


Figure S3 E

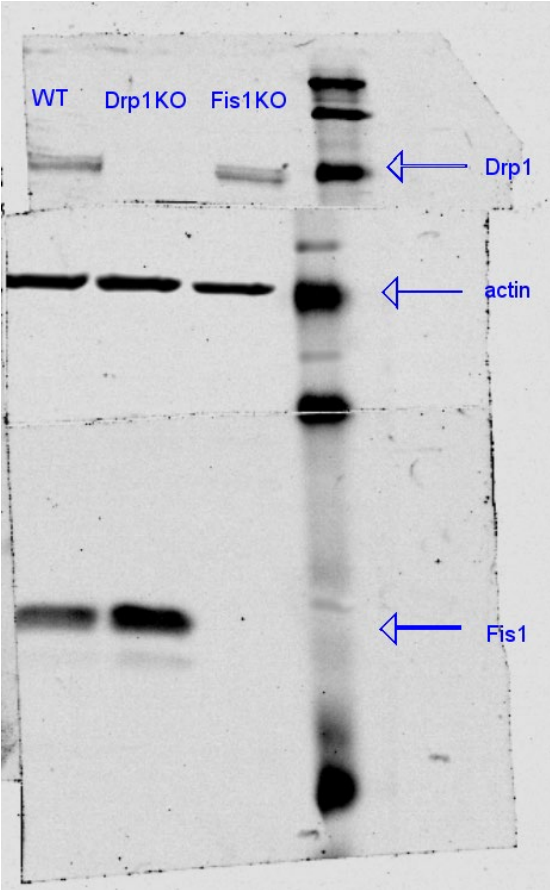
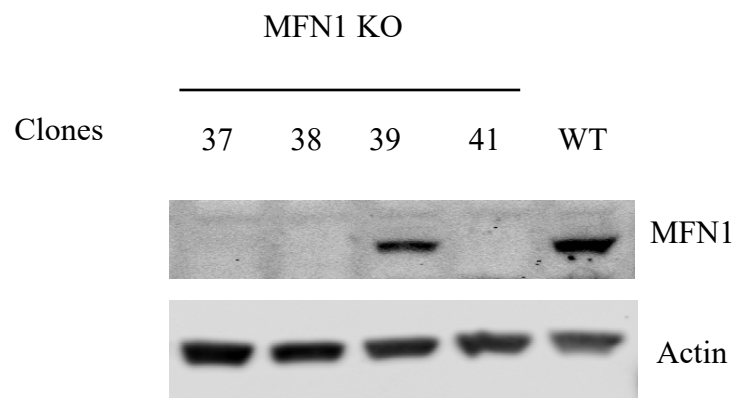
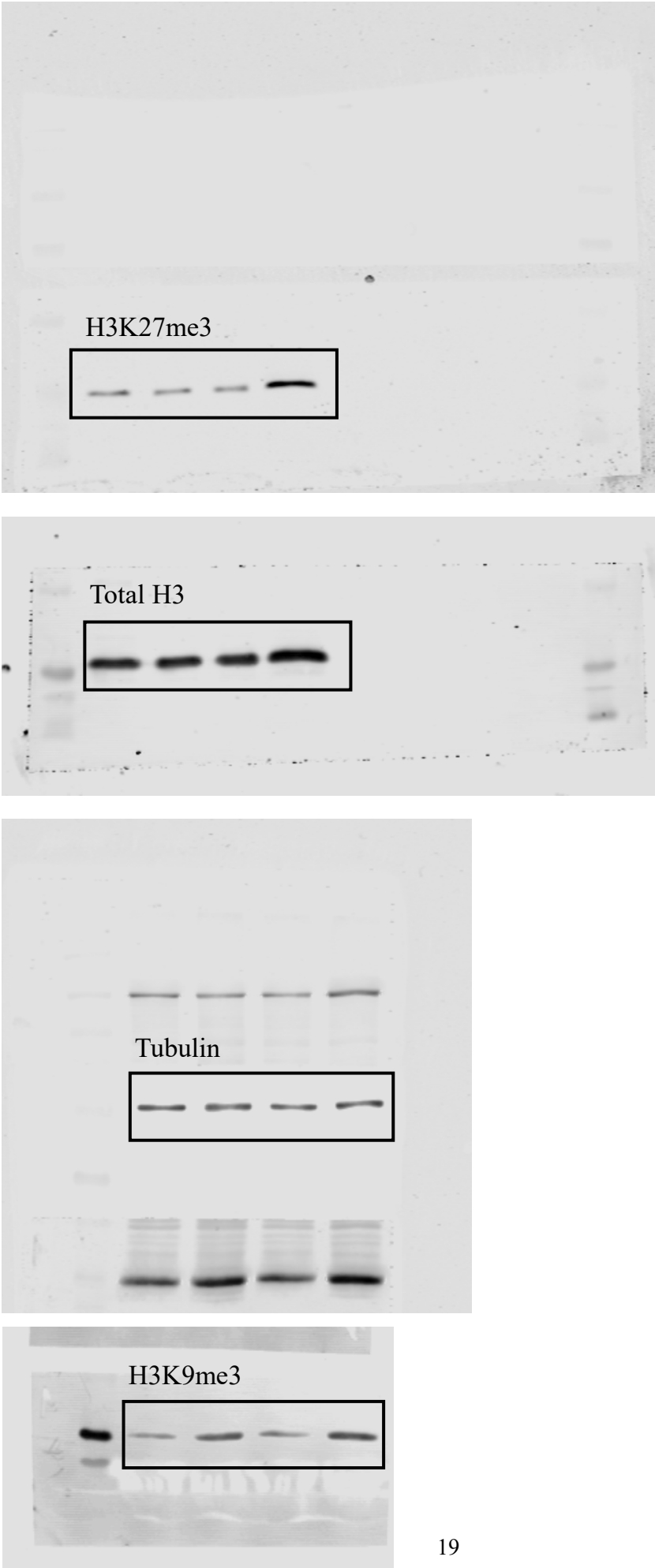


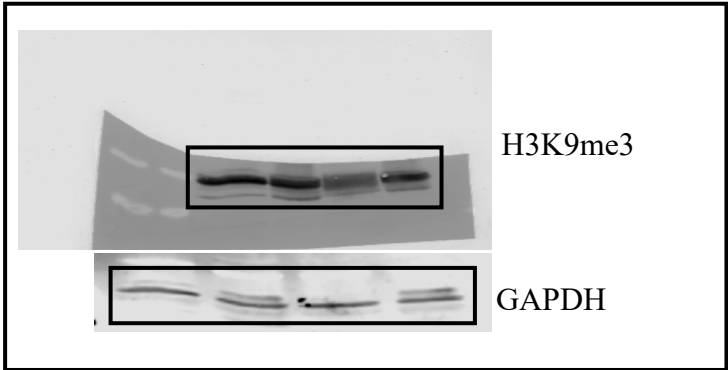


Figure 5 A

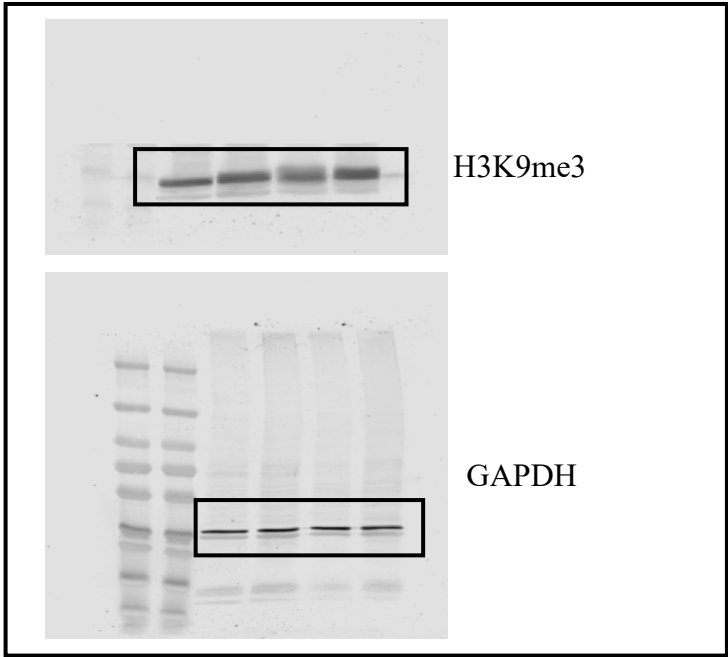


Gels used in Figure 5A quantification

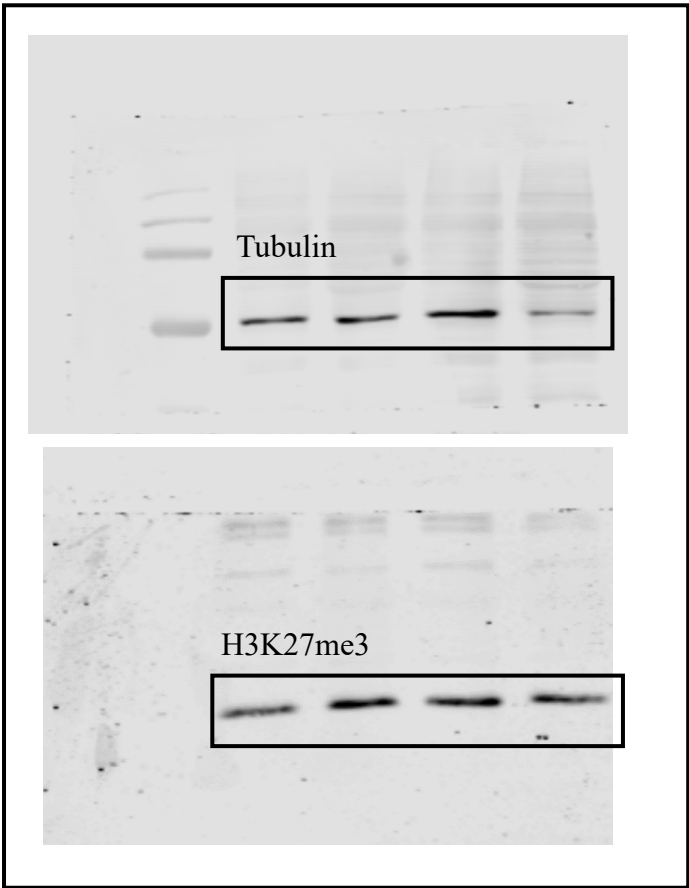
H3K9me3 – gel2



H3K9me3 – gel3



H3K27me3 – gel2



H3K27me3 – gel3

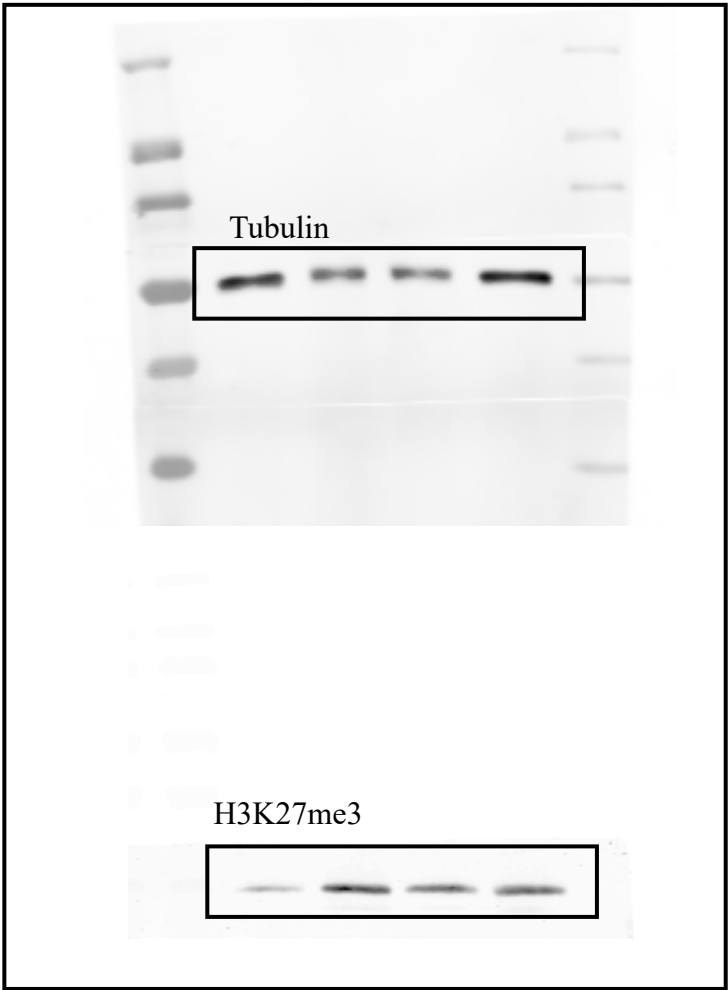
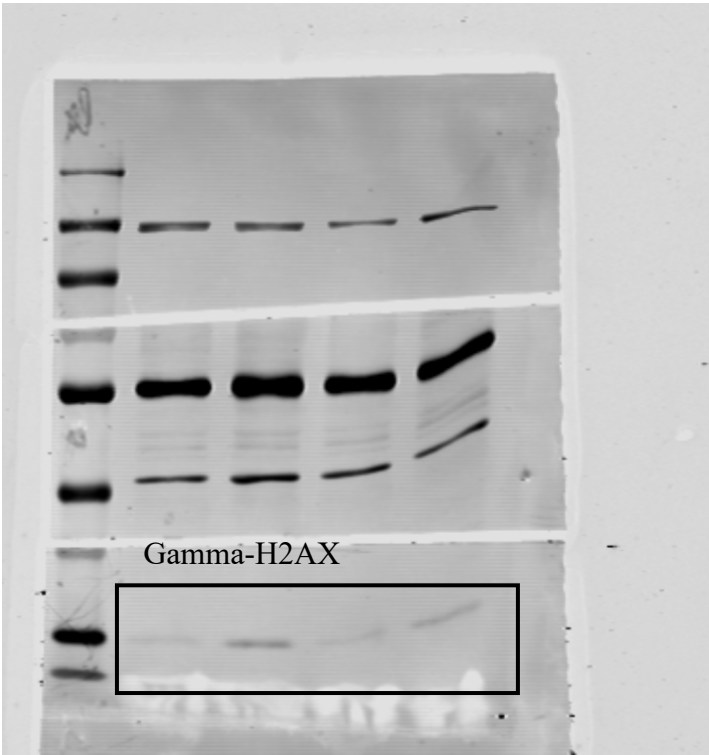


Figure S7 D

High exposure



Low exposure

